Second International Symposium on Marine Propulsors
smp'11, Hamburg, Germany, June 2011

Propeller Design and Propulsion Concepts for Ship Operation in Off-Design Conditions

Thomas Stoye

Flensburger Schiffbau-Gesellschaft (FSG), Flensburg, Germany

ABSTRACT

Ship operators are calling more often for reduced fuel consumption and economic ship operation also in off-design. The versatile operation profile of ship types such as RoRo-vessels are then a challenge for the design of the propeller and for the propulsion concept.

This paper presents aspects on the propeller design and propulsion concept of a ship as well as design methods for the propeller.

Long-term recordings of operation parameters such as pitch setting, propeller revolutions, speed and rudder angle on board of a ship are presented to give an example on a realistic operation profile and its impact on the propeller design.

In addition, design methods for controllable pitch propellers are presented as well as hydrodynamic methods: Calculations with a vortex-lattice method and RANS solutions of a propeller with different pitch settings are compared with model tests and with full-scale measurements.

The prediction of the slipstream of the propeller is also important for the rudder design. An unsteady RANS-calculation of a propeller working in the wake of a ship is compared to PIV-measurements in planes behind the propeller.

Keywords

Propulsion concept, controllable pitch propeller, propeller design, rudder design

1 INTRODUCTION

Ship operators with a fixed regular trade face the possibility to reduce operating costs, if the ship is designed for the requested route. The optimisation of the propulsion concept for a predefined service then offers the possibility to reduce the fuel consumption compared to other vessels on the same trade significantly.

In order to optimise the performance of a propulsion concept for a specified operational spectrum, it is necessary to predict the performance of the propulsion system over the whole variety of operational conditions.

RoRo- and RoPax-vessels are often equipped with diesel-mechanic propulsion and Controllable Pitch Propellers (CPP), giving the vessel the ability for autonomous manoeuvring without tug assistance. Especially in short-sea shipping, this is a widely preferred solution.

However, the ability to control the propeller thrust by pitch setting is also used to control the vessel's speed in sea mode. A shaft generator is then used to generate the ship's electrical power, making it possible to switch off at least one of the auxiliary engines.

In order to assess the efficiency of such an operation, it is necessary to predict the performance of all components, including the behaviour of a CP-propeller with pitch settings different from the design pitch as well as, e.g., the fuel consumption of the main engines.

The performance of the rudder in a propeller slipstream during off-design operation is then also of interest for the assessment of course-keeping and manoeuvring capabilities.

A focus of the present paper is on the development of tools for the hydrodynamic estimation of propulsors and manoeuvring devices in off-design conditions and their practical use in ship design. A further aspect is the interaction with the prime movers, making it possible to assess a propulsion concept as a whole with respect to the total operating costs.

2 FULL-SCALE MEASUREMENTS

Long-term measurements on board of a ship can give a good overview over the operational spectrum in practice. For this purpose, a data recorder has been installed on board of one of FSG's new buildings. The ship is a single-screw RoRo-vessel with 195m LOA, sailing with a design speed of 18.5 knots.

The data recorder has been in use over the period June 2009 – June 2010, when the vessel was operated in regular service between Belgium and Ireland. Beside many other parameters, the ship's speed, the propeller

pitch setting and the specific fuel oil consumption of the main engine has been recorded in time steps of approx. one minute. The vessel is equipped with a shaft generator; the fuel oil consumption therefore represents both the power demand for propulsion and for electric load. The distribution of fuel consumption, propeller pitch setting and speed over ground is shown in Fig. 1. Please note that only conditions, where the ship has been sailing with speeds above 6 knots have been included here. The figure hence represents only operation in sea mode and excludes port manoeuvring. Although the vessel is sailing predominantly in deep water and in areas without speed restrictions, the distribution of speeds show a relatively broad variance in speed, propeller pitch settings and for the fuel consumption.

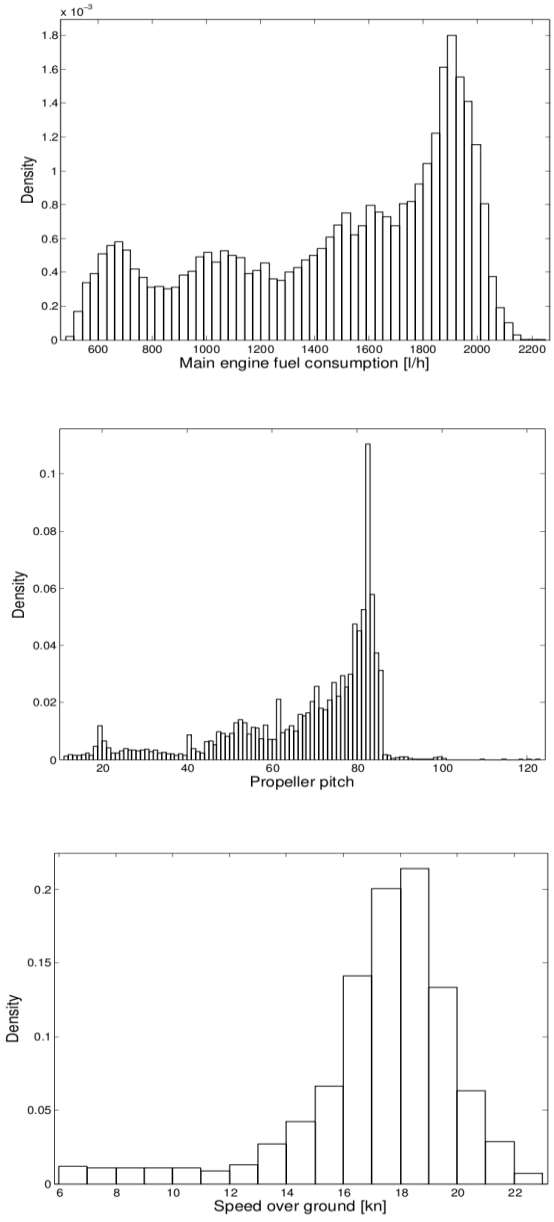

Figure 1: Fuel consumption (top), propeller pitch setting (middle) and speed distribution (bottom) during regular service. The design pitch setting is at 85% of the pitch range

3 CP propeller operation

In order to assess the performance of a CP-propeller in off-design, a detailed description of the propeller blade geometry is necessary. The blade geometry is usually described in either point offset tables along the chord line or, e.g., as a Non-Uniform Rational B-Spline (NURBS). In contrast to a NURBS surface, the description with discrete offset tables has the advantage to use profile series designations. A cubic spline interpolation algorithm in radial direction between the profiles then allows the description of an enclosed surface of the propeller blade.

For CP-operation, the blade is turned around the spindle axis. The blade-describing profile offset tables on discrete radii are then located on different positions on the blade and the profiles defining the blade will have a different shape. Furthermore, e.g., the diameter of the propeller changes if the blade has a significant skew angle.

An algorithm has been developed that allows the turning of the blade by a given angle. In a first step, a delaunay-triangulation generates an enclosed mapping of the blade surface, as shown in Fig. 2. All nodes of the triangulation are then turned by the given angle around the spindle axis. A mapping between the original radii and the new radii allows the identification of the thickness and camber values of the new profiles on the original blade geometry.

This strategy allows both an easy blade design with use of profile series and an accurate geometry description of the blade in CP-operation.

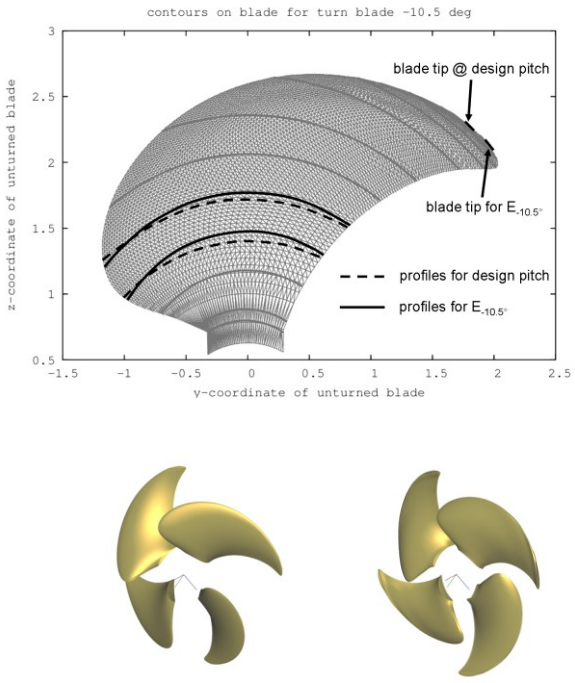

Figure 2: Triangulation and location of blade-defining profiles for different pitch settings (top), 3D-view of the blades (bottom)

4 MESHING

In order to perform RANS calculations that are useable in practice within the standard ship design process, a user interface has been developed for use within FSG's ship design software RDE. This allows the user to perform grid generation and openwater calculations triggered automatically from within the propeller design tool.

In the present case, two different strategies have been implemented for the grid generation, either for Fixed-Pitch Propellers (FPP) or for CPPs:

If the propeller blade is operated with a pitch setting equal or larger than the design pitch setting, it is possible to create a fluid volume as shown in Fig. 3 (left): The volume has a helix shape in the proximity of the blade and is extruded in axial direction up- and downstream. Periodic interfaces are implemented on the fluid boundaries in rotational direction. If the blade area ratio is large (e.g., for FPPs), this topology is a common solution.

However, the use of such a fluid topology is not possible if the pitch setting is decreased: The pitch angles of the blade profiles on the outer radii are small or negative, making it impossible to create a helix-shaped fluid volume around the blade, namely the periodic interfaces will collide with the blade geometry. The alternative strategy is shown in Fig. 3 (right). The area ratio of a CPP is limited, since the blades must not collide when reversing the pitch. The shown fluid volume allows calculations over the whole pitch range of the propeller and is therefore the preferred mesh shape for CP-propellers.

The fluid volume is filled with tetrahedra and with a variable number of prism layers on the propeller blade surface, as shown in Fig. 4. Morgut & Nobile (Morgut 2009) have shown that comparable computation results can be achieved with unstructured meshes compared to a hexa-structured meshing. Especially if the blade design has a high skew angle, a hexa-structured meshing with an automated mesh generation can be difficult. Since the focus of the presented development was a robust design tool for practical ship design, an unstructured meshing strategy has been preferred. In practice, the boundary surfaces of the propeller blade and of the boundaries of the fluid region are generated by RDE, an according batch script is generated and the commercial mesh generation code ANSYS ICEM is then triggered from within RDE.

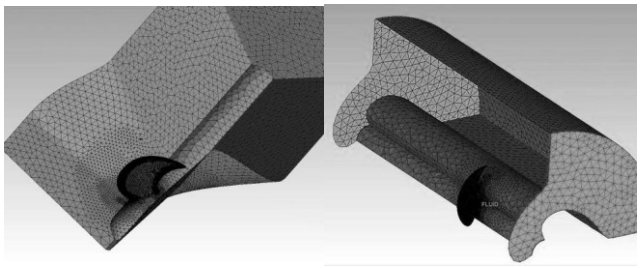

Figure 3: Different meshing strategies for FPPs with high area ratio (left) or CPPs in off-design conditions (right)

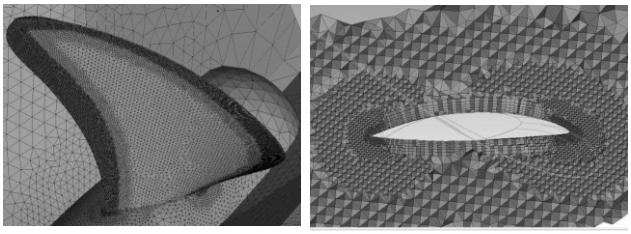

Figure 4: Automatically generated unstructured mesh with prism layers on the blade surface

5 OPENWATER CHARACTERISTICS

Besides the use of RANS calculations, Vortex-Lattice Methods (VLM) are a state of the art technique for propeller design. These methods return reliable results for openwater characteristics, cavitation behaviour, thrust- and torque fluctuations and propeller-induced pressure fluctuations in conditions relatively close to the design condition. For off-design conditions, namely small advance coefficients or CP-propeller pitch settings significantly different from the design pitch, the calculation results are covered with some uncertainty.

Nevertheless, these methods have the advantage of low computation effort (compared to RANS calculations). FSG uses an unsteady vortex-lattice method developed by Streckwall (Streckwall 1997) at Hamburg Ship Model basin (HSVA) for design purposes. RANS computations have been carried out with the commercial solver ANSYS CFX 11.

In order to be able to achieve both fast openwater predictions and accurate results in design and off-design conditions, the use of both VLM and RANS calculations is therefore a practical way to perform propeller blade layout and assessment in ship design.

For validation purposes, extensive model tests have been performed at HSVA for the propeller of the a.m. RoRo-vessel. The propeller has a full-scale diameter of 5.80 m at design pitch. All model tests and calculations have been carried out at a model scale of λ=24.8. The full scale openwater characteristics are then calculated by the method of equivalent profiles (Lerbs 1951).

The thrust and torque coefficients and the openwater efficiency η_0 are shown for advance coefficients J between bollard pull and windmilling condition for the vortex-lattice method and the RANS calculation in comparison to experiments. Within the RANS calculation, the SST (Shear Stress Transport) turbulence model has been used.

The propeller thrust T and the torque Q of the propeller are represented by coefficients K_T and K_Q over the advance coefficient J:

$$J = \frac{v}{nD} \qquad K_T = \frac{T}{\rho n^2 D^4} \qquad K_Q = \frac{Q}{\rho n^2 D^5} \qquad (1)$$

D is the diameter of the propeller in [m], n denominates the propeller revolutions in [1/s], ρ is the density of the fluid in [kg/m^3] and v is the inflow speed [m/s].

Openwater characteristics have been measured for a design pitch setting of 27.29° and for a reduced pitch setting of 16.79° (-10.5° from design pitch).

The openwater characteristics show reasonable agreement of all methods at design pitch and design advance ratio of J=0.8. An uncertainty in the torque prediction of the vortex lattice method can be seen for low advance coefficients, namely if the angle of attack of the blade profiles becomes large.

The RANS method shows reasonable agreement over the whole range of advance coefficients. However, the computational effort is significantly larger with this method.

If the blade pitch setting is reduced by a significant angle, the outer radii will produce reverse thrust, whilst the inner radii generate forward thrust. In such conditions, RANS calculations will produce the most reliable results.

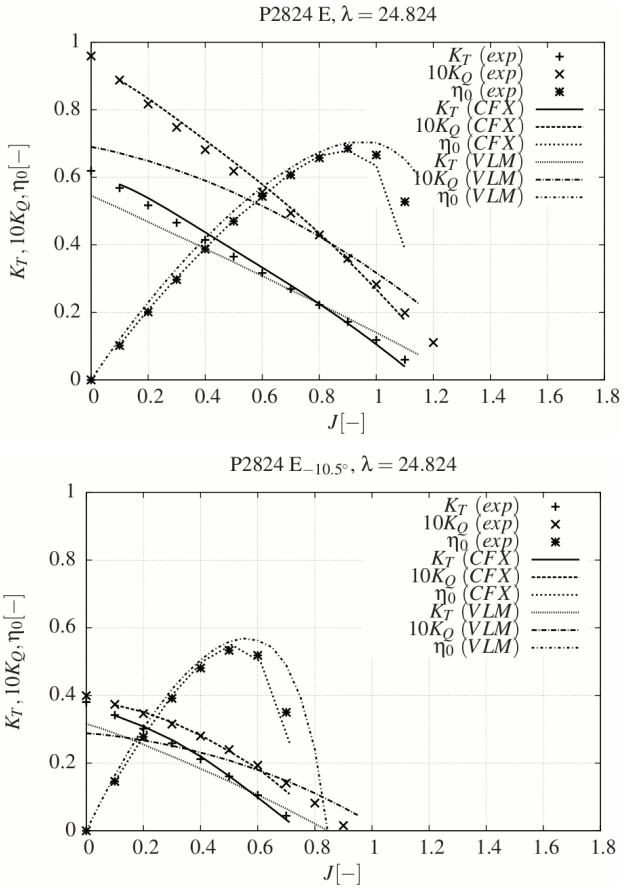

Figure 5: Openwater characteristics for design pitch (top) and reduced pitch setting (bottom)

For this reason, the computed openwater characteristics for a wider operational range have been compared with experiments. The propeller for this investigation has been designed for a twin-screw RoPax-ferry. The propeller blade has a diameter of 5.2m in full scale, whereas all calculations have been performed in a model scale of λ=22.26. The design pitch angle of the propeller is 31.4° and the openwater tests have been carried out with pitch settings of 20° and 60°.

For the representation of thrust and torque over a wider range of inflow conditions, both the advance coefficient J as well as K_T and K_Q will be inadequate. It is therefore common to plot the thrust coefficient c_T and the torque coefficient c_Q over the hydrodynamic pitch angle ß.

The hydrodynamic pitch angle on a radius of 70% of the blade radius is defined as:

$$\beta_{0.7R} = \arctan \frac{V}{0.7\pi nD} \tag{2}$$

whereas the thrust- and torque coefficients include both inflow speed v and propeller revolutions n:

$$c_T = \frac{T}{\frac{\rho}{2}\left[v^2 + (0.7\pi nD)^2\right] A_0} \tag{3}$$

$$c_Q = \frac{Q}{\frac{\rho}{2}\left[v^2 + (0.7\pi nD)^2\right] A_0 D} \tag{4}$$

A_0 denominates the propeller disc area $\pi D^2/4$ in [m^2].

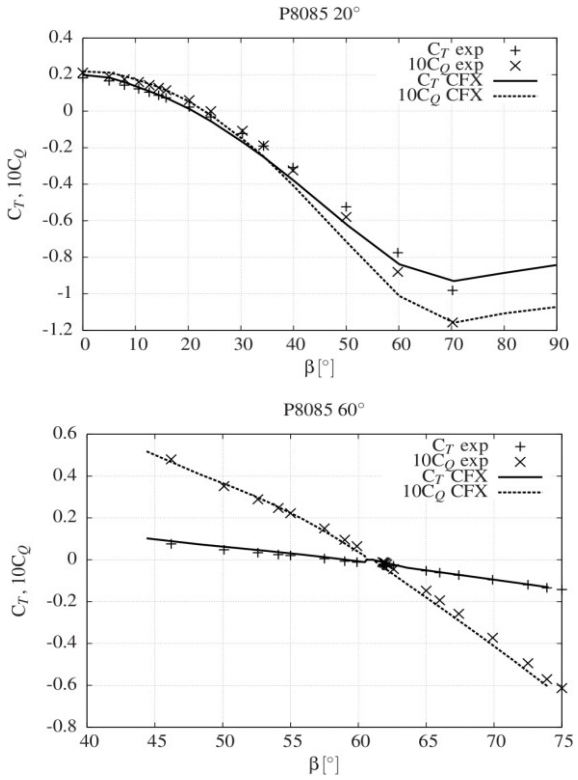

Figure 6: Comparison between calculated and measured openwater characteristics for a pitch setting of 20° (top) and for 60° (bottom)

For the present calculation, the distance of the inlet to the generator plane was 1.0 D, whereas the distance between the outlet and the generator plane was 2.0 D. The ratio between the diameter of the fluid volume and the propeller was 2.5. The mesh for the pitch setting of 20° consists of 592 000 nodes, whereas the mesh for the 60° pitch setting consists of 598 000 nodes. A comparison between measurements and calculations (Fig. 6) shows a reasonable agreement over the whole range of hydrodynamic pitch angles for both pitch settings.

6 PROPULSION CONCEPT

In the following section, an example application of the above presented methods will be given.

The methods have been used to assess different operating modi of a single-screw RoRo-vessel. The ship is intended to operate with a design speed of 20 Kn and an additional reduced speed of 12 Kn for approx. 30% of the sailing time.

The operating modes investigated here include sailing either in const. revolutions or in combinator mode. It is possible to clutch either one or two engines to the shaftline.

The electric load of the ship can be generated by an auxiliary engine with a given specific fuel oil consumption (SFOC) or by a shaft generator, if the engine is running with constant revolutions. This may lead to a better total SFOC and thus to a lower fuel consumption per sailed distance. The investigated combinations of single/twin engine mode, constant revolutions or combinator mode operation, different electric power consumptions for different significant wave heights $H_{1/3}$, inducing different additional resistances are presented in Table 1.

Table 1: Simulated operating modes

Mode	$H_{1/3}$	Engines	Modes	electric power
A	0	2	const. rev.	none
B	0	2	combinator	none
C	0	1	const. rev.	none
D	0	1	combinator	none
E	1.5m	2	const. rev.	none
F	1.5m	2	combinator	none
I	1.5m	2	const. rev.	1700 kW (shaft gen.)
J	1.5m	2	combinator	1700 kW (aux. engine)

Two combinator modes have been defined for single- and twin engine operation, since the pitch setting in single engine operation at maximum lever position is limited by the available power (Fig. 7).

The CPP performance can then be plotted together with the main engine diagram, as shown in Fig. 8.

Depending on the manufacturer and the engine type, the load limit curve give different flexibility in the design of the combinatory diagram. Four-stroke engines generally have a smaller range of revolutions compared to two-stroke engines; the possibility to optimise the combinator mode is hence more limited. Furthermore, required power derived from the combinator diagram should have a certain distance to the load limit curve, leaving sufficient space for operation in heavy sea.

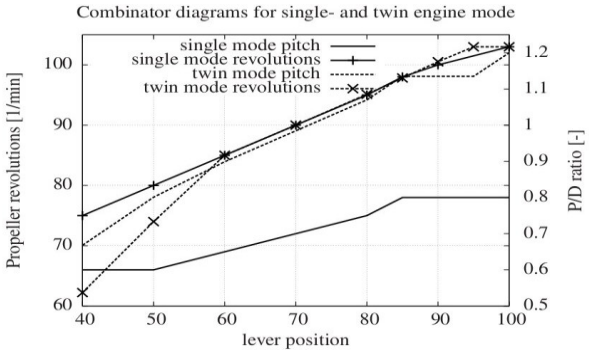

Figure 7: Assignment of propeller pitch and revolutions to the telegraph position

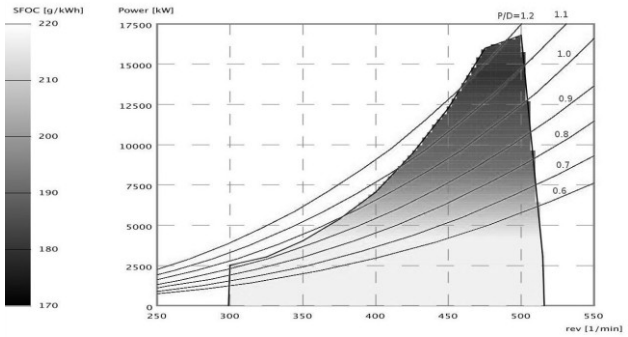

Figure 8: Main engine load limit and specific fuel oil consumption with RANS-computed propeller characteristics for different pitch settings

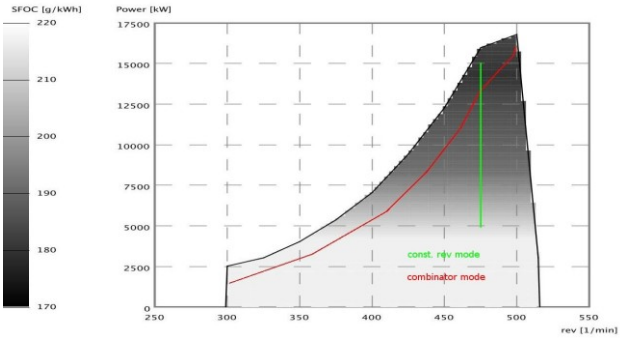

Figure 9: Estimated combinator mode and const. rev. mode (twin engine operation)

From the location of the propeller curve in the main engine diagram, the SFOC can be identified for the specified speed range and the assumed operating

conditions. An estimation of how economic a specific operating mode is can be seen in Fig. 10. It shows the derived total fuel consumption per nautical mile in single- or twin engine mode over the vessel's speed through the water.

When operating with reduced speed, it can clearly be seen that the largest fuel savings can be achieved by switching from const. rev. mode (Mode A and C) to combinator mode (Mode B and D). This is of course only the case if no electric load is present. The single engine operation has only been investigated for calm sea, since the investigated slow speed operation will only be used when sailing through estuary regions without significant weather conditions. For this reason, it is possible to locate the combinator curve for the single engine mode more close to the load limit curve of the main engine.

Fig. 11 shows the fuel oil consumption per distance for twin screw operation with head wind of BFT 4 and a significant wave height $H_{1/3}$ of 1.5m. Without electric load, it can clearly be seen that the combinator mode is again the more efficient compared to the const. rev. mode, the slower the vessel is sailing (Modes E, F).

If there is an electric load present (in the investigated case 1700 kW), there is an optimum speed of approx. 12 knots with the lowest fuel consumption per distance, when operated in const. rev mode (Mode I). During operation in combinator mode (Mode J), the electrical power is generated by the auxiliary engine, consuming 220 g/kWh. In that case, the optimum fuel consumption can be found even at a lower speed. For an electric load of 1700 kW, it can be concluded that operation in combinator mode with the auxiliary engine producing the electric power is more efficient for speeds below 14 kn, whereas the use of the shaft generator is the more economic solution for higher speeds in terms of fuel consumption.

This coincides also with the fact that a reduced pitch setting in const. rev. mode is always combined with a certain danger of onset of face side cavitation.

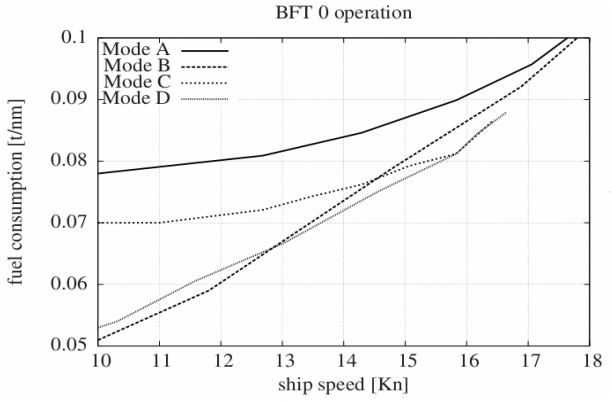

Figure 10: Comparison of fuel consumption for single- and twin engine operation in const. revolutions or combinator mode

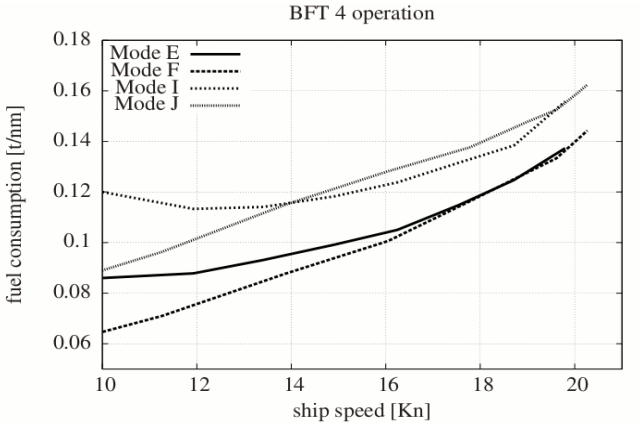

Figure 11: Comparison of fuel consumption for const. revolutions or combinator mode and different electric loads

7 RUDDER INFLOW CONDITIONS

The requirements on the manoeuvring and course-keeping capabilities are relatively high for RoRo- and RoPax-vessels. The design of the rudder is therefore of importance in early design stages, since it strongly interacts with the propeller and the ship's hull.

The inflow conditions to the rudder have been investigated for operation in off-design conditions. The a.m. RANS methods have been used to assess the flow conditions around the rudder in off-design.

The rudder has been designed as a so-called twist-flow rudder with a costa bulb. The profiles are fitted with a certain camber such that the average angle of attack of the rudder profiles is as small as possible when operating in the propeller slipstream.

The calculations presented here are compared to PIV (Particle Image Velocimetry) measurements in the cavitation tunnel (HYKAT) of HSVA. The vessel investigated is the a.m. RoRo-vessel in service between Belgium and Ireland. In the present case, an unsteady calculation has been performed. The mesh consists of four unstructured meshes of each blade and a mesh around the rudder, connected via a generalized grid interface (GGI).

As inlet boundary condition, the measured wakefield of the ship has been used. The wakefield has originally been measured in the propeller plane, whereas the inlet in the computation was located at 0.7R in front of the propeller plane. The calculation is therefore not fully equivalent to the model test conditions. Moreover, the innermost radius of the measured wakefield was 0.38R, whereas the hub has a radius of 0.27R. This gap has been extrapolated.

The mesh consists of 3.5 Mio. cells with prism layers on the propeller and rudder blades. The topology of the mesh is presented in Fig. 12.

Model tests have been carried out with a reduced pitch setting from the design pitch of 5° and a rudder angle of 10° to starboard. A comparison of the velocities in a plane of 0.6R below the propeller hub is shown in Fig. 13. The colours indicate the magnitude of velocity in the xy-plane

relative to the homogenous inflow speed in front of the ship (3.55 m/s). The images represent a phase angle of 30° of the propeller key blade relative to the 12 o'clock position. Please note that the images are taken from below the ship's hull.

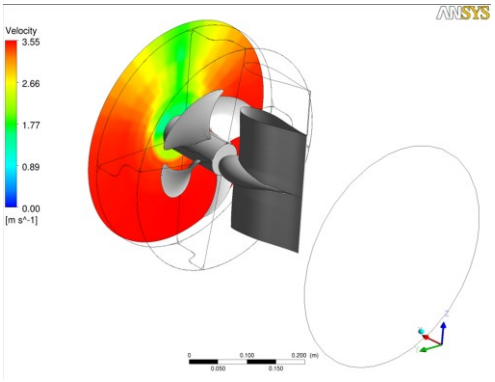

Figure 12: Inflow conditions and model setup

In the vicinity of the propeller and rudder blades, the velocities show reasonable agreement, but at larger distances from the geometries, detailed flow characteristics such as tip vortices cannot be found in the computation anymore. This is due to the fact that the hybrid meshing has been generated relatively coarse downstream of the propeller.

The unsteady flow characteristics are represented in Fig. 14: For three different phase angles, the flow angle α in the xy-plane is shown over the relative blade radius on a horizontal line at the location x=0.4R downstream of the propeller. The calculations show good agreement with the measurements on the outer radii whereas the angles are overpredicted on the inner radii. This might be due to the fact that the wakefield is not represented correctly on the inner radii. It is noteworthy that in both experiment and calculation, the inflow angle to the rudder has a fluctuation of up to 9° during a single passage of the propeller blade. This should be accounted for during the design of the rudder profiles in order to guarantee cavitation-free operation in all relevant design- and off-design conditions.

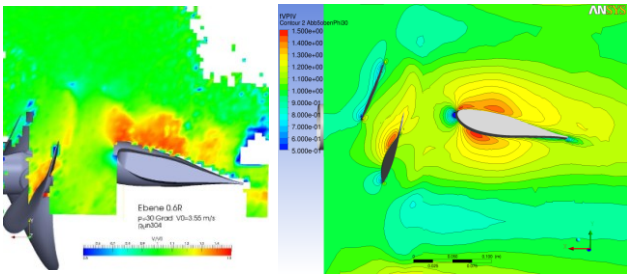

Figure 13: Comparison of PIV measurements (left) and computations (right): The magnitude of velocities relative to the inflow velocity in a horizontal plane for a blade phase angle of 30°

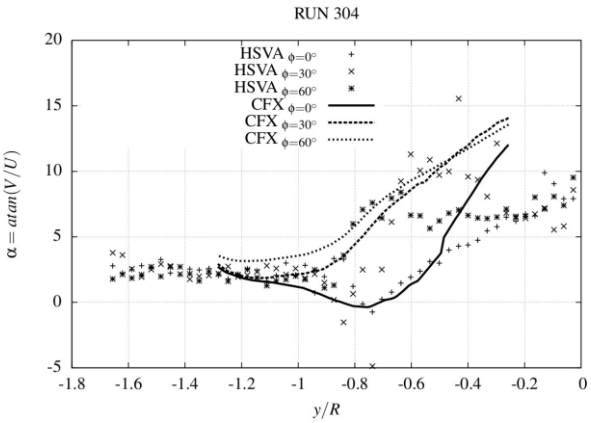

Figure 14: Comparison of computational flow angles (CFX) in a horizontal plane and PIV measurements (HSVA)

8 CONCLUSION

The main objective of this paper has been to demonstrate the use of hydrodynamic design tools for the assessment of propulsion concepts.

Long-term measurements on board of a RoRo-ship show the necessity to take the versatile operational profile into account during the layout of the propulsion concept.

In order to be able to design the propeller for the given design- and off-design conditions, it is necessary to be able to design the blade in an easy way and at the same time to extract the blade geometry for pitch settings different from the design pitch.

The propeller can then be assessed with hydrodynamic calculations. Both VLM and RANS calculation results are presented here, giving an overview over the applicability of both methods. The use of both RANS and VLM then allows the computation of the CPP performance in off-design conditions with a sufficient accuracy for the ship's design stage.

The definition of the combinator mode then allows the assessment of the total performance of the prime movers and auxiliary engines in different operating conditions in terms of fuel consumption. The propeller and propulsion evaluation presented in this paper is therefore an integral part of the ship design.

The presented calculation results of the flow around the rudder show that RANS calculations can also contribute to the evaluation of the rudder design in off-design conditions.

ACKNOWLEDGEMENT

Model tests, full scale observations, software developments and hydrodynamic calculations were sponsored by the German ministry of economics (BMWi) within the research project OFF-DESIGN. All model tests mentioned have been performed at HSVA. Long-term onboard measurements have been conducted with support and on board of a ship of the Belgian operator COBELFRET.

REFERENCES

Abbott, I. H. & von Doenhoff, A. E. (1959). Theory of Wing Sections. Dover Publications Inc.

Abdel-Maksoud, M. & Müller, S.-B. (2004). 'Scale Effect on the Hydrodynamic Characteristics of Propellers'. 25th Duisburg Colloquium, Duisburg, Germany.

Carlton, J. S. (2007). Marine Propellers and Propulsion. 2nd ed. Elsevier Ltd.

Greitsch, L. & Eljardt, G. (2009). 'Simulation of Lifetime Operating Conditions as Input Parameters for CFD Calculations and Design Evaluation'. Numerical Towing Tank Symposium, Cortona, Italy.

Lerbs, H. (1951). 'On the Effect of Scale and Roughness on Free Running Propellers'. Journal of the American Society of Naval Engineers (ASME).

Lücke, T. & Streckwall, H. (2009). 'Cavitation Research on a Very Large Semi Spade Rudder'. Proceedings of The First International Symposium on Marine Propulsors, Trondheim, Norway.

Morgut, M. & Nobile, E. (2009). 'Comparison of Hexa-Structured and Hybrid-Unstructured Meshing Approaches for Numerical Prediction of the Flow Around Marine Propellers'. Proceedings of The First International Symposium on Marine Propulsors, Trondheim, Norway.

Streckwall, H. (1997). 'Description of a Vortex-Lattice Method for Propellers in Steady and Non Steady Flow'. HSVA Report **CFD 18/97**.